

K. KONOPKA\*, L. LITYŃSKA-DOBRZYŃSKA\*\*, J. DUTKIEWICZ\*\*

## SEM AND TEM STUDIES OF $\text{NiAl}_2\text{O}_4$ SPINEL PHASE DISTRIBUTION IN ALUMINA MATRIX

### BADANIA SEM I TEM ROZMIESZCZENIA FAZY SPINELOWEJ $\text{NiAl}_2\text{O}_4$ W OSNOWIE $\text{Al}_2\text{O}_3$

Methods of enhancing of mechanical properties of ceramic–metal composites, particularly fracture toughness by introducing dispersed metal particles such as W, Mo, Ni, Al, etc to a ceramic matrix are well known. However, the dependence of the microstructures, especially interfaces, on the properties of composites is not well understood yet. Moreover, the ceramic–metal interfaces play a crucial role in tailoring the composite properties.

In this paper we examine the alumina matrix composite with  $\text{NiAl}_2\text{O}_4$  spinel phase and present the SEM and TEM studies of spinel distribution, size and crystallographic orientation. The composites were prepared by sintering  $\text{Al}_2\text{O}_3$  and Ni powders below the melting point of Ni in argon. During the process of sintering the spinel phase appeared. It was not homogeneously distributed in the alumina matrix. The spinel phase areas were linked together and constituted an almost continuous form. We observed that the distribution and size of spinel influenced the fracture toughness of the composite.

*Keywords:* spinel phase,  $\text{NiAl}_2\text{O}_4$ , ceramic–metal composites, SEM, TEM

Wprowadzenie do osnowy ceramicznej cząstek metalu np. W, Mo, Ni, Al, a także innych zapewnia wzrost odporności na pękanie uzyskanych kompozytów. Jest to już dobrze znany fakt, jednakże nie do końca opisany jest wpływ powierzchni międzyfazowych na właściwości kompozytów.

W pracy analizowano kompozyt  $\text{Al}_2\text{O}_3$ -Ni z udziałem spinelu  $\text{NiAl}_2\text{O}_4$ . Obserwacje SEM i TEM ujawniły niejednorodne rozmieszczenie spinelu w objętości materiału. Opisano orientację krystalograficzną, grubość i kształt fazy spinelowej. Powstająca na granicach między cząstkami niklu a osnową  $\text{Al}_2\text{O}_3$  spinel tworzy prawie ciągłe układy łączące sąsiednie cząstki niklu. Stwierdzono wpływ fazy  $\text{NiAl}_2\text{O}_4$  na odporność na pękanie kompozytów.

### 1. Introduction

The potential for using alumina in engineering applications is high due to a high-hardness and high – compression strength to weight ratio and good properties at elevated temperatures. However, the brittleness of alumina limits its applications. The enhancement of mechanical properties, particularly fracture toughness is achieved by introducing dispersed metal particles to a ceramic matrix [1-4]. One of these, metal particles that were added was nickel and this resulted in improved fracture toughness even up to 12 MPa  $\text{m}^{0.5}$  [4]. The oxidation behavior of the Ni-toughened alumina is important and must be considered. As a consequence of the oxidation process the new phases can appear in a composite microstructure. The nickel inclusions on the surface area are the first to be oxidized and the NiO is formed. As the oxidation proceeds, the NiO reacts with the alumina matrix and the spinel phase  $\text{NiAl}_2\text{O}_4$  appears [1, 6]. Due to the fact that the oxidation takes place first by the interface reaction between oxygen gas and the exposed nickel particles at the composite surface and then it is controlled by diffusion of Ni ions through the grain boundaries of  $\text{Al}_2\text{O}_3$  and through the spinel layer [1, 7], the distribution

of spinel phase is not uniform in bulk materials. Spinel phase influences the mechanical properties of composite [1, 7, 8] and therefore it is important to characterize its distribution and morphology as well as crystallographic orientation.

The work is continuation of the SEM and TEM characterization of the composites, some of whose results were presented in the paper [8]. In this paper the SEM and TEM studies of spinel distribution, size and crystallographic orientation are presented. Also, the influence of  $\text{NiAl}_2\text{O}_4$  on the crack propagation and fracture toughness of composite is discussed.

### 2. Experimental procedures

The composites (97.7 wt %  $\text{Al}_2\text{O}_3$ + 2.3 wt % Ni) were prepared by powder compaction. Alumina powder ( $\alpha$ - $\text{Al}_2\text{O}_3$ ) TM-DAR (Tamei Chemical Corporation Co. Ltd., Japan) with purity of 99.99% (the particle size ranging from 0.2 to 0.5  $\mu\text{m}$ ) and nickel powder (Aldrich Co) with a purity of 99.8% and a particle size of 3  $\mu\text{m}$  were used.

The preparation procedure is as follows: mixing the powders in a ball mill with an addition of ethanol for 1h, drying

\* WARSAW UNIVERSITY OF TECHNOLOGY, FACULTY OF MATERIALS SCIENCE AND ENGINEERING, WOŁOSKA 141, 02-507 WARSAW, POLAND

\*\* INSTITUTE OF METALLURGY AND MATERIALS SCIENCE POLISH ACADEMY OF SCIENCES, 30-059 CRACOW, 25 REYMONTA ST., POLAND

at a 60°C for 24h, preparing the samples for the pressing operation by adding 2g of the PSA (5%) binder to 10g of the powder mixture. Powder compacts with cylindrical shape and diameter of about 8 mm and a height of 5 mm were formed by pressing uniaxially at 50 MPa. The sintering was carried out at a temperature of 1450°C in an argon atmosphere for 1h.

The density of the specimens was determined by the Archimedes method. The microstructure of the composite was examined using Philips PW 1830 X-ray diffractometer (XRD) with CuK<sub>α1,54</sub> radiation. Microstructural characterization used scanning electron microscope Hitachi S-2600 (SEM) and FEI transmission electron microscope Tecnai G<sup>2</sup> (TEM) operating at 200 kV equipped with a high-angle annular dark field scanning transmission detector (HAADF/STEM) combined with EDAX energy dispersive X-ray (EDX) microanalyser. Thin foils of composite interfaces for TEM were obtained using FEI FIB instrument.

The microhardness was tested using hardness test machine Future-Tech FV-700e. The fracture toughness K<sub>IC</sub> was estimated using the crack length generated by an indenter using the Niihara equation [9]. The thickness and the size of the spinel phase was estimated from the SEM images. To this aim the computer program for the stereological analysis of obtained images "MicroMeter" was used [9].

**3. Results and discussion**

The macro-observation of Al<sub>2</sub>O<sub>3</sub>-Ni composite samples after the process of sintering revealed that argon atmosphere did not prevent oxidation. This sample was of a blue colour (Fig. 1A). An X-ray phase analysis of the edge part of the sample confirmed that spinel phase was formed (Fig. 1B). In the central part of sample (after cutting) the alumina, Ni and spinel phase were detected (Fig. 1C).

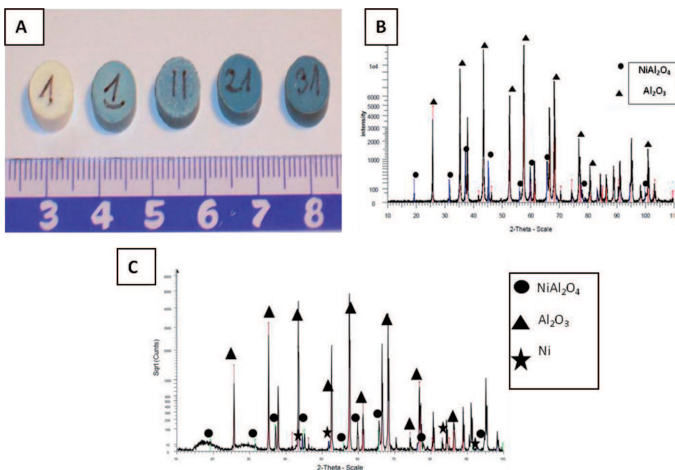


Fig. 1. A) Macro- images of samples, composite sample in blue color, reference sample -100% Al<sub>2</sub>O<sub>3</sub> – white color, B) X-ray phase analysis from the edge part of composite sample, phases Al<sub>2</sub>O<sub>3</sub> and NiAl<sub>2</sub>O<sub>4</sub>, C) X-ray phase analysis from the central part of composite sample, phases Ni, Al<sub>2</sub>O<sub>3</sub> and NiAl<sub>2</sub>O<sub>4</sub>

The SEM observation of the longitudinal section of the sample showed that near the edge of the sample the area of spinel phase distributed in alumina matrix is visible (Fig. 2A).

Moving from the edge to the central part of the sample the Ni particles surrounded by the spinel phase and Ni particles in alumina matrix were observed (Fig 2B). The changes in the distribution of spinel phase, that is the decrease of the spinel phase amount in the microstructure, together with the distance from the edge of the sample to the central part (Fig. 2A) indicated that spinel formation is more intensive at the surface. This can result from oxygen absorption of the sample surface and the fact that Ni particles are embedded deep in the matrix and can suffer from various degrees of partial oxidation. These relationships of spinel formation were earlier studied [1, 5] also by authors [8].

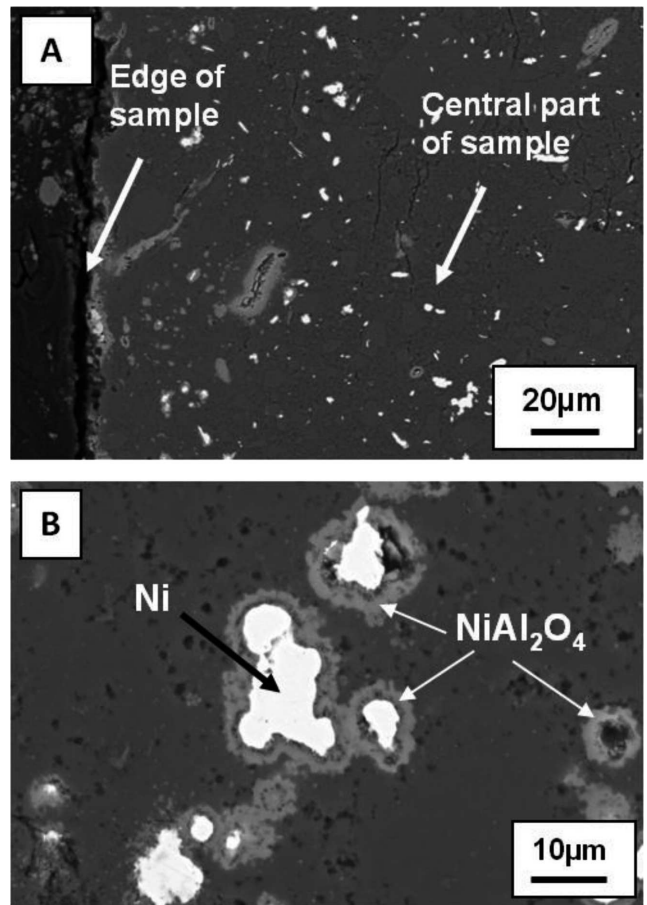
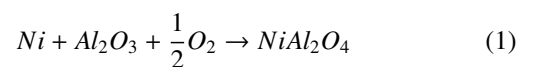


Fig. 2. SEM images of Al<sub>2</sub>O<sub>3</sub>+2,3 wt. % Ni composite : A) the longitudinal section of the composite B) central part of the sample

From the point of view of the mechanical properties of composites, spinel amount contribution and their size and shape, as well as its distribution in the microstructure are crucial [1, 7, 8]. In order to calculate the amount of the spinel in the composite the following reaction of spinel formation was assumed [5]:



To calculate the mass of elements, the wt % of powders Ni and Al<sub>2</sub>O<sub>3</sub> needed to prepare the sample were used. The obtained value of NiAl<sub>2</sub>O<sub>4</sub> amount in the composite was 6.92 wt %.

The SEM observations revealed an oval shape of spinel phase. However, the thickness of the spinel around the Ni particles is not uniform (Fig. 2B). The estimated average thickness

of spinel phase forming a ring around the Ni particles is equal to  $1.35 \mu\text{m}$ . The average diameter is equal to  $2.7 \mu\text{m}$  and the maximum value is up to  $10.2 \mu\text{m}$ . The average surface area of spinel is equal to  $31.49 \mu\text{m}^2$ . According to the work [11] the size of the spinel phase shows about a 6-fold increase in volume in comparison to the size of the initial Ni particles. Our own calculations of the volume of spinel phase formed around the spherical Ni particles yielded an 8-fold increase in the value [12]. The calculated values of amount and thickness of spinel suggest that its existence at the microstructure of composite can have a significant influence on the hardness and the fracture toughness.

Moreover, the spinel phase areas have characteristic holes, resembling “doughnuts” (Fig. 2B). This shape of  $\text{NiAl}_2\text{O}_4$  may result from the difference in the values of the thermal expansion coefficient [12]. Another feature of spinel is that the spinel grains linked the neighbour Ni particles as a “bridge”. As a consequence, they were anchored between the alumina grains. These is noticeable in STEM-HAADF observations (Fig. 3).

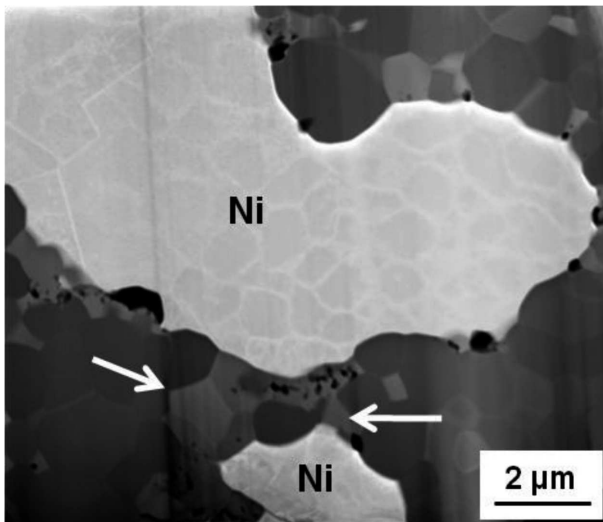


Fig. 3. STEM-HAADF image of the composite  $\text{Al}_2\text{O}_3+2.3 \text{ wt. } \% \text{ Ni}$

Two Ni particles (visible as bright areas) are surrounded by oxide or spinel grains. The spinel  $\text{NiAl}_2\text{O}_4$  phase could be easily recognized because of the lighter contrast compared to the oxide (the contrast in the HAADF detector depends on the atomic number of the elements which form the phase). Spinel is not uniformly distributed along the nickel grains; in some areas spinel grains link the neighboring nickel particles (marked on the Fig. 3 by arrows), although there are also nickel/oxide interfaces where spinel does not form. It could also be seen that the holes, visible as dark areas near the Ni particles, occur only close to spinel grains or between them. Figure 4 presents a TEM bright-field micrograph of the interface of  $\text{Al}_2\text{O}_3$ , Ni and spinel and a corresponding diffraction pattern taken from the area of Ni and spinel phases. Inside the nickel particle a high density of dislocations and subgrains, which probably formed as a result of deformation during the process of production, is visible. The pores and holes are present only in the spinel grains unlike in to the oxide structure. Based on the presented diffraction pattern the following crystallographic relationship between Ni and spinel (S) grain (with dark con-

trast) could be determined:  $[112] \text{ S} \parallel [015] \text{ Ni}$  and  $(40\bar{2}) \text{ S} \parallel (200) \text{ Ni}$ .

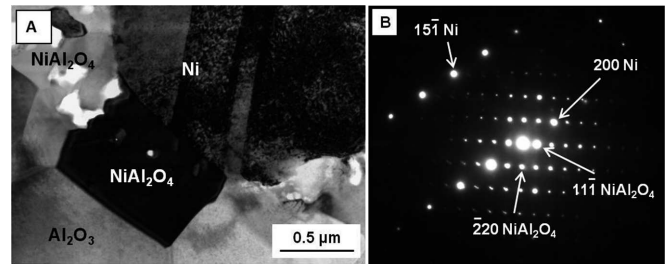


Fig. 4. TEM bright-field image (A) and corresponding selected area diffraction pattern (B) of the interface of the Ni and  $\text{NiAl}_2\text{O}_4$  grains –  $[015]$  zone axis of Ni and  $[112]$  zone axis of spinel

As a consequence of the characteristic distribution, shape and amount of spinel in composites, their hardness is changed. The microhardness  $\text{HV}_{0.02}$  measured at the edge of the sample where the spinel was present in alumina matrix was equal to 856 and the fracture toughness  $K_{IC}$  was equal to  $5.4 \pm 0.4 \text{ [MPa}\cdot\text{m}^{1/2}]$ . For the central part of the sample where the Ni particles were surrounded by the spinel as well as the spinel area and the Ni particles were separated by the alumina matrix, the average value of  $\text{HV}_{0.02}$  was equal to 458 and  $K_{IC}$   $6.1 \pm 0.3 \text{ [MPa}\cdot\text{m}^{1/2}]$ . The obtained results confirmed that the spinel phase has an influence on the hardness and the fracture toughness.

The highest value of hardness at the edge of the sample where only two phases  $\text{NiAl}_2\text{O}_4$  and  $\text{Al}_2\text{O}_3$  were detected resulted from the high hardness of spinel. Moreover, the thermal expansion mismatch between the phases at the interfaces creates a stress field which further enhances strengthening of the composite. As a consequence, the value of  $K_{IC}$  should decrease. The fact that we did not observed decrease in this value in comparison with the reference sample 100% alumina where  $K_{IC}$  is equal to  $5.5 \pm 0.4 \text{ [MPa}\cdot\text{m}^{1/2}]$  is a result of crack propagation through the interfaces spinel/alumina which enhanced the fracture toughness.

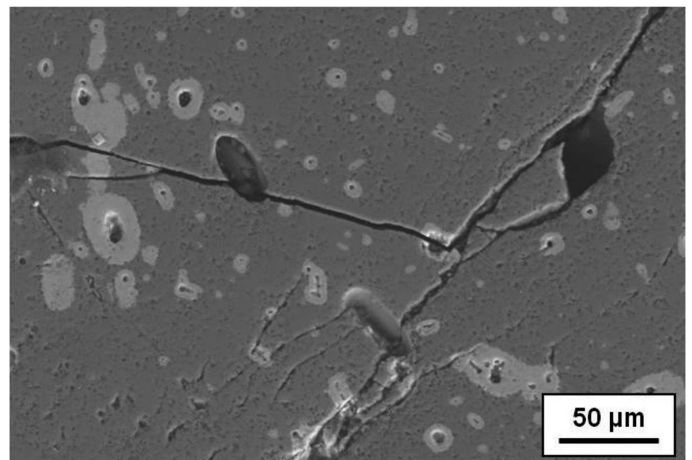


Fig. 5. SEM image of  $\text{Al}_2\text{O}_3+2,3 \text{ wt. } \% \text{ Ni}$  composite, crack propagation

In the central part of the sample the increase of the  $K_{IC}$  value is the effect of the presence of interfaces: Ni/ $\text{NiAl}_2\text{O}_4$ , Ni/ $\text{Al}_2\text{O}_3$ /  $\text{NiAl}_2\text{O}_4$ / $\text{Al}_2\text{O}_3$ . For weak strength interfaces be-



tween Ni particles and alumina matrix and between Ni and spinel, we observed the crack deflection and pulling out of metal particles as shown in the micrograph in Fig. 5, which also was suggested in [13]. Moreover, deformation of Ni particles and its bridging are highly probable [2]. Strong interfaces developed between spinel and alumina matrix result in a crack cleavage or cause its movement along the perimeter of the interface as can be seen in Fig. 5. All the above processes dissipate the crack propagation energy, which results in the increase in the fracture toughness of composites.

#### 4. Conclusions

In the microstructure of the composites nickel-toughened alumina prepared by mixing of powders and then sintering below the melting point of Ni in argon, the spinel phase appeared. The spinel phase distribution is not homogeneous. In the outer part of the sample only the spinel phase located in alumina matrix was observed. The “doughnuts” shape of  $\text{NiAl}_2\text{O}_4$  may result from the difference in the values of the thermal expansion coefficient.

In the central part of the sample above the spinel area also the Ni particles surrounded by spinel rings with different thickness are identified. Moreover, the spinel grains linked the neighbour Ni particles as a “bridge”. As a consequence, they were anchored between the alumina grains.

Based on the TEM investigations the following crystallographic relationship between Ni and spinel (S) grain could be determined:  $[112] \text{S} \parallel [015] \text{Ni}$  and  $(40\bar{2}) \text{S} \parallel (200) \text{Ni}$ . The estimated amount of  $\text{NiAl}_2\text{O}_4$  in microstructure is equal to 6.92 wt%. The existence of spinel phase, its amount and its distribution in the microstructure of composite influences its mechanical properties.

In the outer part of the sample  $\text{NiAl}_2\text{O}_4$  causes the increase in the hardness. In the central region of the sample the existence of the Ni particles will contribute to the lower hardness. In both parts of the sample the increase in fracture toughness was noticed. The increase in the  $K_{IC}$  value is an effect of the presence of interfaces:  $\text{Ni}/\text{NiAl}_2\text{O}_4$ ,  $\text{Ni}/\text{Al}_2\text{O}_3/\text{NiAl}_2\text{O}_4/\text{Al}_2\text{O}_3$ . Higher strength interfaces developed between the spinel and the alumina matrix cause a crack cleavage or its movement along the perimeter of the interface. The de-

formation of Ni particles and the crack bridging were also observed.

#### Acknowledgements

The results presented in this paper have been obtained within the project “KomCerMet” (contract no. POIG.01.03.01-14-013/08-00 with the Polish Ministry of Science and Higher Education) in the framework of the Operational Programme Innovative Economy 2007-2013.

Authors would like to thank Prof. M. Szafran and his Group from Warsaw University of Technology, Faculty of Chemistry for help in preparing the samples and MSc. J. Właszczuk and MSc. A. Miazga from Warsaw University of Technology, Faculty of Materials Science and Engineering for help in the experiments.

#### REFERENCES

- [1] T.C. Wang, R.Z. Chen, W.H. Tuan, *Journal of the European Ceramic Society* **23**, 927 (2003).
- [2] W.H. Tuan, R.J. Brook, *Journal of the European Ceramic Society* **6**, 31 (1990).
- [3] T. Sekino, K. Niihara, *Nanostructured Materials* **6**, 663 (1995).
- [4] W.G. Fahrenholtz, D.T. Ellerby, R.E. Loehman, *J. Am. Ceram. Soc.* **83**, 1279 (2000).
- [5] W.H. Tuan, M.C. Lin, H.H. Wu, *Ceramics International* **21**, 221 (1995).
- [6] P.H. Bolt, S.F. Lobner, J.W. Geus, F.H.P.M. Habraken, *Applied Surface Science* **89**, 339 (1995).
- [7] F.S. Pettit, E.H. Randklev, E.J. Elten, *J. Am. Ceram. Soc.* **60**, 105 (1977).
- [8] K. Konopka, L. Lityńska-Dobrzyńska, J. Dutkiewicz, *Solid State Phenomena* **186**, 222 (2012).
- [9] T. Wejrzanowski, Special computer program for image analysis-Micrometer. MSc Thesis, Warsaw University of Technology, Warsaw, Poland, 2000.
- [10] K. Niihara, R. Morena, D.P.H. Hasselmann, *J. Mater. Sci. Let.* **1**, 13 (1982).
- [11] M. Lieberthal, W.D. Kaplan, *Materials Science and Engineering A* **302**, 83 (2001).
- [12] K. Konopka, *Inżynieria Materiałowa* **3**, 457 (2010).
- [13] K. Konopka, A. Miazga, J. Właszczuk, *Kompozyty* **11**, 197 (2011).